Hindawi
International Transactions on Electrical Energy Systems
Volume 2022, Article ID 8256908, 17 pages
https://doi.org/10.1155/2022/8256908

Research Article

Multiobjective Salp Swarm Algorithm Approach for Transmission Congestion Management

Anjali Agrawal,[1] **Seema N. Pandey**,[2] **Laxmi Srivastava**,[3] **Pratima Walde**,[4] **R. K. Saket**,[5] **and Baseem Khan**[6]

[1]*Department of Electrical and Electronics Engineering, Noida Institute of Engineering & Technology, Greater Noida, UP, India*
[2]*Department of Electrical Engineering, Dr. Bhim Rao Ambedkar Polytechnic College, Gwalior, MP, India*
[3]*Department of Electrical Engineering, Madhav Institute of Technology and Science, Gwalior, MP, India*
[4]*Department of Electrical Engineering, Sharda University, Greater Noida, UP, India*
[5]*Department of Electrical Engineering, Indian Institute of Technology (BHU), Varanasi, UP, India*
[6]*Department of Electrical & Computer Engineering, Hawassa University, Hawassa, Ethiopia*

Correspondence should be addressed to Baseem Khan; baseem.khan04@gmail.com

Received 23 June 2022; Revised 3 November 2022; Accepted 19 November 2022; Published 7 December 2022

Academic Editor: Kin Cheong Sou

In the newly emerged electric supply industry, the profit maximizing tendency of market participants has developed the problem of transmission congestion as the most crucial issue. This paper proposes a multiobjective salp swarm algorithm (MOSSA) approach for transmission congestion management (CM), implementing demand side management activities. For this, demand response (DR) and distributed generation (DG) have been employed. For willingly reducing the demand, demand response has been called by providing appropriate financial incentives that supports in releasing the congestion over critical lines. Distributed generation implementing wind plant as renewable independent power producer (RIPP) has also been included in order to reduce the load curtailment of responsive customers to manage transmission congestion. The proposed incentive-based demand response and distributed generation approach of CM, has been framed with various strategies employing different thermal limits over transmission lines and has resulted into significant reduction in congestion and in-turn improvement of transmission reliability margin. Diversity has been obtained in multiobjective optimization by taking two and three objective functions, respectively (minimization of overall operational cost, CO_2 emission, and line loading). The by-products of the proposed algorithm for multiobjective optimization are minimized demand reduction, optimum size, and location of DG. To examine the proposed approach, it has been implemented on IEEE 30-bus system and a bigger power system IEEE 118-bus system; as well as the proposed technique of MOSSA has been compared and found better than reported methods and two other meta heuristic algorithms (multiobjective modified sperm swarm optimization and multiobjective adoptive rat swarm optimization).

1. Introduction

Transmission congestion management has now become one of the most important issues of present deregulated power market [1]. In this open access power market scenario for getting more profit margins from the market, problem of congestion is enlarging day by day [2, 3]. To mitigate congestion various CM methods have been reported from the generator side and from the demand side.

Generation rescheduling (GR) [4–6] and enhancement of ATC through FACTS devices [7] are the generation side management. In early stage of deregulation, customers were not directly involved in market operations and security maintaining issues. Only independent system operator and regulatory utilities were responsible for managing energy systems. If customers (who are increasing the load) are well informed about the reliability and security issues, then they may have participated efficiently in maintaining operation of

power markets. In newly developed power market environment, an incentive-based demand response program along with energy storage system and distributed generation has been suggested to achieve a flexible energy hub in electricity market [8] and DSM (demand side management) has proved itself as more promising tool for congestion management [9]. Thus, targeted DSM along with distributed generation (DG) can be an effective alternative of CM [10]. Under DSM, customers adjust their demands on the basis of awareness for energy conservation or by getting financial incentives [11–13].

DR is all about reducing the demand for alleviating congestion [14]. However, the inspiration of any commodity business is to increase the consumption as much as possible, which is conflicting towards DR. Thus, decrement in demand offered by DR has to be kept in limit to increase avoid customer facility. So in order to limit the DR amount, distributed generation (DG) has to be added for managing congestion [15].

Distributed generation can be accomplished by any energy sources such as wind, solar, diesel, bio-gas, natural gas [16–21]. Out of these sources, wind (renewable energy sources) is supposed to be the most advisable distributed generation plant [22].

In the present paper, the problem of CM has been formulated under the multiobjective optimization framework. However, in the literature most of the times CM problem has been solved with double objective optimization framework [23, 24]; while in present approach overall operating cost, emission of CO_2 and transmission line loading have been considered as objective functions.

The traditional techniques of solving multiobjective optimization problems have been outmoded because of their sluggishness due to large number of iterations, complexity, stagnation, and full of approximations. However, the involvement of evolutionary algorithms such as differential evolution and particle swarm has overcome these issues and encourage the researchers to employ the multiobjective optimization in the field of power system [25]. The training of efficient deep reinforcement learning agents for in-the-moment life-cycle production optimization was carried out by the authors in [26]. For a parallel inverter system, the authors of [27] introduced a unique droop control mechanism to maximize photovoltaic power output. The gated spatial-temporal graph neural network-dependent short-term load forecasting for wide-area multiple buses was given by the authors in [28]. The distribution of centrally switched fault current limiters in the transmission system was given in [29]. The multistate approach for improving transmission network resilience against short-circuits faults brought on by extreme weather occurrences were presented by authors in [30]. The split-core magnetoelectric current sensor and wireless current measuring application were presented in [31]. The review of deep learning applications in frequency analysis and regulation of contemporary power systems was offered by the authors in [32]. Authors in [33] presented a hierarchical multiobjective optimal planning model for an active distribution system that takes demand-side responsiveness and distributed generation into account. The estimate of the probabilistic energy flow for the regional integrated energy system taking into account the cross-system failures was published in [34].

An energy storage system based multiobjective congestion management has been presented by using GAMS software [35] and genetic algorithm [36]. Hence, in the present work the recently developed multiobjective salp swarm algorithm (MOSSA) [37] with number of strategies has been proposed for solving multiobjective optimization-based CM problem.

The performance of MOSSA for CM has been compared with two other meta heuristic algorithms, namely, multiobjective modified sperm swarm optimization and multi-objective adoptive rat swarm optimization. The prescribed work in this paper have been examined on IEEE 30-bus system and IEEE 118-bus system and compared with methods reported (same power system) in literature [23, 38]. The proposed approach of congestion management has been compared with similar reported methods shown in Table 1.

The contribution of the paper is as follows:

(1) The problem of congestion management has been handled as multiobjective and simulated by implementing multiobjective salp swarm algorithm for simultaneous optimization of three objective functions

(2) These three objective functions (minimization of overall operational cost, CO_2 emission, and line loading) have not been found in the literature simultaneously

(3) Transmission congestion has been relieved by employing generation rescheduling, demand response, and wind plant simultaneously

(4) The performance of MOSSA has been compared and found better than two other nature inspired algorithms, namely, multiobjective modified sperm swarm optimization and multiobjective adoptive rat swarm optimization

(5) Seven specific cases have been taken first time which have not been considered earlier

The structure of the present paper is as follows: in the second section, multiobjective CM problem has been formulated with three objective functions along with all constraints. Third section describes the proposed multiobjective salp swarm algorithm, adoptive rat swarm optimization, and modified sperm swarm optimization. In the fourth section, numerical results are presented and analysed for IEEE 30-bus system and IEEE 118-bus system. In the fifth section, this paper has been concluded.

2. Problem Formulation

2.1. Objective Functions. Three objective functions for multiobjective CM problem have been formulated as follows:

2.1.1. Minimization of Overall Operational Cost. In the present work, overall operation cost minimization has been achieved by minimizing cost of generation, cost of demand

Table 1: Comparison of proposed CM approach with the reported methods.

Reported methodologies	Congestion management strategy	Advantages	Disadvantages	Reference
NSGA-II/DE	DG	Multiobjective	Transmission expansion	[1]
Fitness distance ratio-PSO and fuzzy adaptive-PSO	GR	CM in hybrid power market	Single objective	[4]
Gravitational search algorithm	ATC enhancement	CM with TCSC	Cost not included/single objective	[7]
GAMS software	DR	CM with renewable energy source	Cost not included/Single objective	[13]
CPLEX (MATLAB)	DR	CM with renewable energy source	Cost not included/single objective	[14]
Differential evolution	DG	CM with renewable energy source	Cost not included/single objective	[15]
Matpower toolbox	DG	CM based on flow gate marginal price	single objective	[16]
GA based	DG	LMP difference based CM	Generation cost not included	[17]
DE-PSO	DG	CM with renewable energy source	Multiobjective problem handled as single objective	[18]
Flower pollination	DG	CM with renewable energy source	Multiobjective problem handled as single objective	[19]
MOPSO	DRP	2-objective functions	High demand response	[23]
Jaya algorithm	Transmission switching/ DR	Hybrid power system	All transmission lines cannot be switched off	[24]
GAMS software	Optimal energy storage system charging	Multiobjective	Cost and emission are in single objective/load shedding	[35]
Hybrid bacterial foraging and nelder–mead algorithm	TCSC placement	2-objective functions	Multiobjective problem handled as single objective	[38]
MATPOWER (MATLAB)	TCSC placement	CM with renewable energy source	Cost not included/single objective	[39]
MOSSA [proposed]	DR/RIPP	3-objective functions/CM with renewable energy source		[Proposed]

response, and cost of distributed generation. The above said objective functions are as follows:

(1) Generation Cost. Conventional generation cost C_G ($/hr) can be written as follows [23]:

$$C_G = \sum_{i=1}^{N_G} \left(a_i + b_i P_{G_i} + c_i P_{G_i}^2\right) \quad i = 1, 2, 3 \ldots\ldots\ldots N_G, \tag{1}$$

where a_i, b_i, and c_i are the cost coefficients of i^{th} generating unit.

(2) Cost of Renewable Independent Power Producer (RIPP). In this paper wind plant has been considered as renewable independent power producer playing a role of DG. Cost function (C_{RIPP}) of RIPP can be expressed as follows [39]:

$$\begin{aligned} C_{\text{RIPP}} &= \Psi \times P_{WP} \frac{\$}{hr}, \\ P_{WP} &= \frac{1}{2} \text{air}_d \times W_t \times \eta_{WP} \times v_{\text{wind}}^3. \end{aligned} \tag{2}$$

where Ψ represents cost of wind power generation ($/MWhr), air_d (kg/m^3) is presenting the air density factor, W_t (m^2) representing the swept area of wind turbine, η_{WP} shows the overall efficiency of wind plant, and v_{wind} (m/sec) shows the wind velocity.

(3) Demand Response Cost. Demand response program (DRP) is the process in which responsive customers are convinced to reduce their demands to bring down the loading over critical transmission lines. Some appropriate monetary incentive ($/MW) are offered to these customers to curtail their demands. This is termed as DR cost. Demand response (DR) cost ($/hr) can be written as follows [20]:

$$C_{DR} = \sum_{k=1}^{N_{DR}} \mu_k, \tag{3}$$

where μ_k is the DR cost for k^{th} responsive customer in $/hr and $N_{DR} \in N_B$. Equation (3) indicates that DR cost minimization is actually the minimization of load reduction or minimization of incentive paid to the customers.

Demand response cost of k^{th} responsive customer can be expressed as follows [23]:

$$\mu_k = \text{INC} \times \left(d_{0_k} - d_k\right). \tag{4}$$

Customers participated in DRP that not modify the required demand adjustment, then they have to be penalised with certain penalty. Penalty can be formulated as follows [12]:

$$\begin{aligned}\mathscr{L}_k &= \text{PEN} \times \left[LR_k - \left(d_{0_k} - d_k\right)\right],\\ \mathscr{L}_k &= \text{PEN} \times \left[LR_k - Ad_k\right],\end{aligned} \tag{5}$$

where $\mathscr{L}_k$ is the penalizing cost bore by k^{th} responsive customer in \$/hr. The reduced demand d_k can be expressed as follows [11]:

$$d_k = d_{0_k} \times \left[1 + \varepsilon \times \left\{\frac{(EP_{DR} - EP_0) + (\text{INC} - \text{PEN})}{EP_0}\right\}\right]. \tag{6}$$

First objective function cost can be given as follows:

$$F_1 = \text{minimize}\{C_G + C_{DR} + C_{\text{RIPP}}\}. \tag{7}$$

2.1.2. CO_2 Emission. The problem of CO_2 emission minimization can be modelled as follows:

$$F_2 = \text{minimize}\,(E) = \text{minimize} \sum_{i=1}^{N_G} \left(\alpha_i + \beta_i P_{G_i} + \gamma_i P_{G_i}^2\right). \tag{8}$$

2.1.3. Minimization of Line's Maximum Loading. This objective function is purposely involved in solving the present CM problem. Loading highly congested line has been considered for this objective function and can be given by the following equation:

$$F_3 = \text{minimize}\left(\max S_l\right), \tag{9}$$

where l is the most congested transmission line and $l \in \text{N}_{\text{BR}}$.

2.2. Constraints. For the proposed multiobjective CM problem all constraints can be given as follows:

2.2.1. Equality Constraints. Power balance can be expressed as follows [23]:

$$\begin{aligned}P_{G_i} - P_{D_i} - V_i \sum_{j=1}^{N_B} V_j \left[G_{ij}\cos\left(\delta_i - \delta_j\right) + B_{ij}\sin\left(\delta_i - \delta_j\right)\right] = 0,\\ Q_{G_i} - Q_{D_i} - V_i \sum_{j=1}^{N_B} V_j \left[G_{ij}\sin\left(\delta_i - \delta_j\right) + B_{ij}\cos\left(\delta_i - \delta_j\right)\right] = 0,\end{aligned} \tag{10}$$

where G_{ij} and B_{ij} are the transmission conductance and susceptance between bus i and j, respectively, and $\delta_i\,\delta_j$ are the voltage angles at i^{th} and j^{th} buses, respectively.

2.2.2. Inequality Constraints. On the basis of minimum and maximum limits of power system inequality constraints can be given as follows:

(a) Inequality constraints for generators [23].

$$\begin{aligned}P_{G_i}^{\min} \le P_{G_i} \le P_{G_i}^{\max}, \quad i = 1, 2, 3 \ldots\ldots N_G,\\ Q_{G_i}^{\min} \le Q_{G_i} \le Q_{G_i}^{\max}, \quad i = 1, 2, 3 \ldots\ldots N_G,\\ V_{G_i}^{\min} \le V_{G_i} \le V_{G_i}^{\max}, \quad i = 1, 2, 3 \ldots\ldots N_G.\end{aligned} \tag{11}$$

(b) Inequality constraints for security [23].

$$\begin{aligned}V_i^{\min} \le V_i \le V_i^{\text{Max}}, \quad i = 1, 2, 3 \ldots\ldots\ldots\ldots\ldots N_{LB},\\ S_{\max_l} \ge S_l, \quad l = 1, 2, 3 \ldots\ldots\ldots\ldots\ldots N_{BR}.\end{aligned} \tag{12}$$

(c) Demand response constraints.

Financial incentive paid to the k^{th} responsive customer for ensuring his contribution in managing congestion must be bounded within a lower and upper limit. This is the cost for demand response and has to be kept restricted to maintain DR within limits. This can be written as follows [20]:

$$\begin{aligned}\mu_k^{\min} \le \mu_k \le \mu_k^{\max}, \quad k = 1, 2, 3 \ldots\ldots N_{DR},\\ DR_k^{\min} \le DR_k \le DR_k^{\max}, \quad k = 1, 2, 3 \ldots\ldots N_{DR}.\end{aligned} \tag{13}$$

(d) Constraints for wind plant [30].

$$P_{WP}^{\min} \le P_{WP} \le P_{WP}^{\max}. \tag{14}$$

3. Optimization Algorithms

In the present work CM has been handled as multiobjective optimization problem. Hence, simultaneous minimization of all objective function have been carried out by the Multiobjective slap swarm algorithm, multiobjective modified sperm swarm optimization, and multiobjective adoptive rat swarm optimization.

3.1. Multiobjective Salp Swarm Algorithm. In the present work multiobjective salp swarm algorithm proposed by [37] has been employed to solve MOO-based CM problem. Salps belong to the category of Salpidae and have a barrel shaped transparent body seems such as jelly fish. Their forward movement is just such as jet propulsion. The mathematical model for solving optimization problems is based on the most interesting swarming behaviour of salps. Salps made swarm which is called salp chain. The first salp at the front of the chain is called leader and the rest of the salps are called followers. Similarly to other swarm-based multiobjective techniques, MOSSA also has multidimensional search and objective space.

Updated position of leader salp using three parameters c_1, c_2, and c_3, can be given as follows:

$$x_j^1 = \begin{cases} F_j + c_1\left(\left(ub_j - lb_j\right)c_2 + lb_j\right), & c_3 \ge 0,\\ F_j - c_1\left(\left(ub_j - lb_j\right)c_2 + lb_j\right), & c_3 < 0,\end{cases} \tag{15}$$

where $x1/j$ presents the position of leader salp in j^{th} search dimension, F_j is the target food source in j^{th} dimension, ub_j

and lb_j are the upper and lower bounds of variables in j^{th} dimension.

Parameters c_2 and c_3 are generated randomly between [0, 1] while c_1 is very important parameter which provides a balance between exploration and exploitation during optimization and depends upon size of iterations. It can be given as follows:

$$c_1 = 2e^{-(-4k/K)^2}, \tag{16}$$

where k and K are the iteration count and maximum number of iterations, respectively.

Follower salps update their position on the basis of updated position of leader salp and can be given as follows:

$$x_j^i = \frac{1}{2}\left(x_j^i + x_j^{i-1}\right), \tag{17}$$

where $i \geq 2$ indicating follower salps and x_j^i is the i^{th} follower salp in j^{th} dimension.

Multiobjective salp swarm optimization contains multiple optimum solution that can be termed as nondominated solutions. For extracting good compromise and best solutions among the set of nondominated solutions, membership function μ_i can be given as follows [25]:

$$\mu_i = \begin{cases} 1, & F_i < F_i^{\min}, \\ \dfrac{F_i^{\max} - F_i}{F_i^{\max} - F_i^{\min}}, & F_i^{\min} < F_i < F_i^{\max}, \\ 0, & F_i \geq F_i^{\max}. \end{cases} \tag{18}$$

Normalized fuzzy membership function $\mu_{i,j}$ for multiple solutions can be given as follows:

$$\mu_{i,j} = \frac{\sum_{i=1}^{N_{\text{obj}}} W_i \mu_i}{\sum_{j=1}^{N_{\text{REPO}}} \sum_{i=1}^{N_{\text{obj}}} W_i \mu_i}. \tag{19}$$

3.2. Adoptive Rat Swarm Optimization (ARSO). The rat swarm optimization is a nature inspired meta-heuristic technique Figure 1 and it is based on following and attacking (social painful) behaviour of rats [40]. In this algorithm rat agents explore the optimum solution in search space and update their position on the basis of best rat position such as other swarm based optimization techniques. Its performance can be improved by adoptive version of RSO in which initial population is updated on the basis of opposition based learning [40]. The steps for the ARSO are as follows [40]:

Step 1. Generate initial rat population by using the following equation randomly under the upper and lower limits of search space.

$$x^k = x^{k^{\min}} + \text{rand} * \left(x^{k^{\max}} - x^{k^{\min}}\right), \quad k = 1, 2, 3 \ldots . M. \tag{20}$$

where $x^{k^{\min}}$ and $x^{k^{\max}}$ are the lower and upper bounds of search space, respectively, and M is the population size.

Step 2. Select initial parameters A, R, and C.

Step 3. Generate opposite number based solutions ($\overrightarrow{x}^k$) by using the following equation for these initial population on the basis of opposite number concept.

$$\overrightarrow{x}^k = \left(x^{k^{\max}} - x^{k^{\min}}\right) - x^k, \quad k = 1, 2, 3 \ldots . . . . M. \tag{21}$$

Step 4. Evaluate fitness function for both initial population $f(x^k)$ and opposite number based solutions $f(\overrightarrow{x}^k)$. If $f(\overrightarrow{x}^k)$ is better than $f(x^k)$, then replace x^k by $\overrightarrow{x}^k$ for starting the optimization. Now, rat agents explores best solution in search space.

Step 5. During optimization to avoid local minima worst solution, we replaced it by a best (new) solution in each iteration using following equation:

$$x^{\text{worst}} = \begin{cases} \text{rand}^1 * \overrightarrow{P}^r(x), & \text{if rand}^2 \leq 0.5, \\ \left(x^{k^{\max}} - x^{k^{\min}}\right) - x^k, & \text{if rand}^2 > 0.5, \end{cases} \tag{22}$$

where x^{worst} is the worst solution, $P^r(x)$ is the best solution, and rand^1 and rand^2 are the random numbers between 0 and 1.

Step 6. Selected population update their position using the following equation by getting information from the greatest search agent (rat population) to get the optimal solution.

$$\overrightarrow{P}^r(x+1) = \left|\overrightarrow{P}^r(x) - \overrightarrow{P}\right|. \tag{23}$$

where $\overrightarrow{P}^r(x+1)$ = denotes updated position of rat population, $\overrightarrow{P}^r(x)$ is the position of greatest search agent, and $\overrightarrow{P}$ can be evaluated by using the following equation:

$$\overrightarrow{P} = A * \overrightarrow{P}^k(x) + C * \left(\overrightarrow{P}^r(x) - \overrightarrow{P}^k(x)\right), \tag{24}$$

where $\overrightarrow{P}^k(x)$ is the position of k^{th} rat population and parameters A and C can be given by the following equations, respectively.

$$A = R - q * \left(\frac{R}{\text{iter}^{\max}}\right), \quad q = 1, 2, 3 \ldots . \text{iter}^{\max}, \tag{25}$$

where $\text{iter}^{\max}$ is the maximum iteration number and q is the current iteration number.

$$C = 2 * \text{rand}, \tag{26}$$

where R and C is a random number between [1, 5] and [0, 2].

Step 7. Stop if stopping criteria has been reached otherwise go to step 5.

Step 8. Optimum solution obtained.

3.3. Modified Sperm Swarm Optimization (MSSO). Sperm swarm optimization is inspired by sperm swarm behaviour during fertilization of ovum [41]. In this algorithm a set of

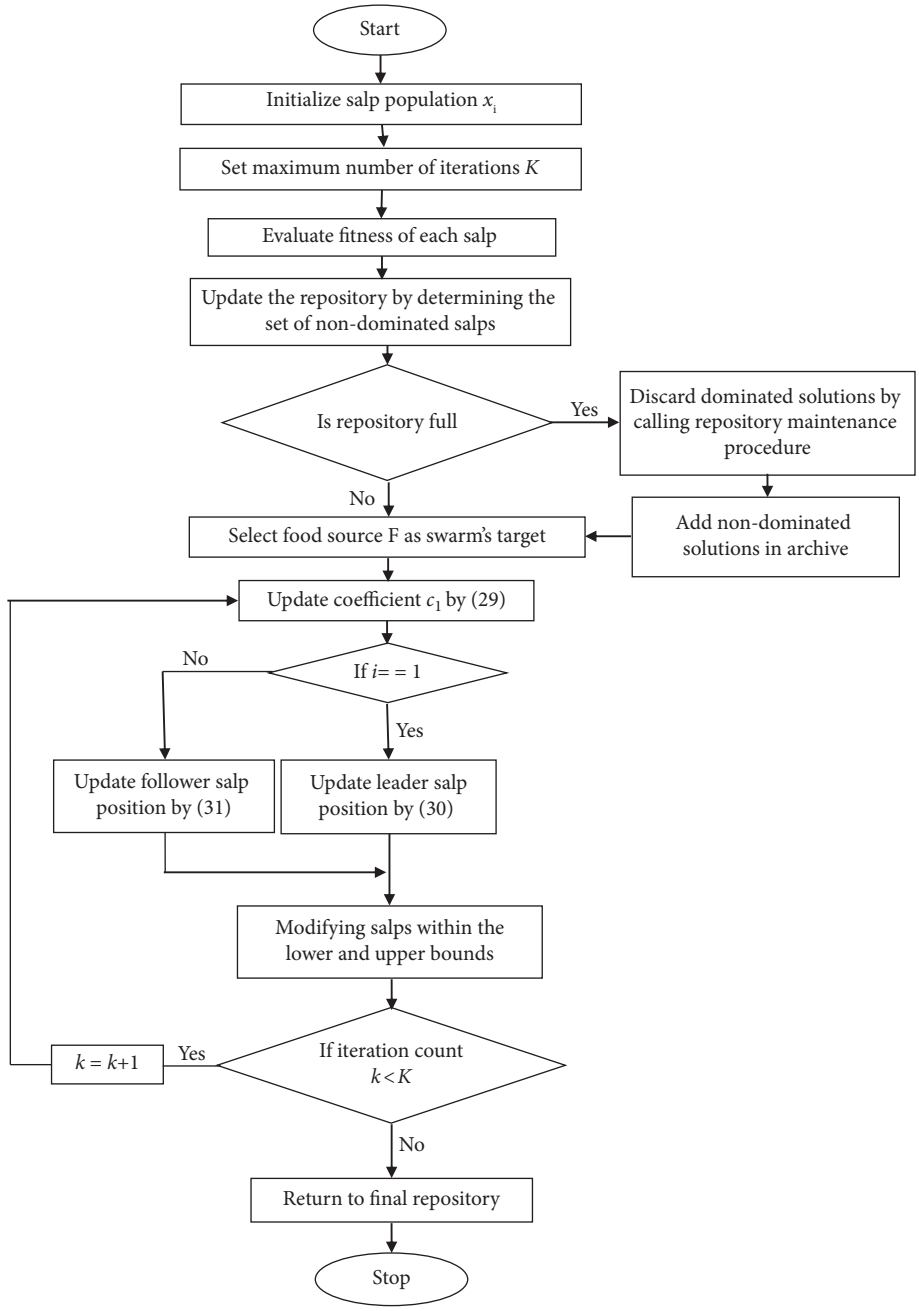

Figure 1: Flow chart of proposed MOSSA algorithm.

searching agents of sperm (potential solutions) levitate in search space to explore and achieve the optimum solution. The searching agents update their position on basis of their personal best and global best position of sperm swarm. Mathematically searching sperms update their position according to following equation:

$$x_k(t+1) = x_k(t) + v_k(t), \tag{27}$$

where $v_k(t)$ is the current velocity of k^{th} sperm and t is the iteration number. To avoid the premature convergence and improving the performance of MSSO chaotic dynamics are integrated.

Hence, damping factor has been modified by the following equation:

$$CD = \theta * 100 * e^{\left(-20*\text{iter}/\text{iter}_{\max}\right)}. \tag{28}$$

Finally, the current velocity of k^{th} sperm can be given as follows [41]:

$$\begin{aligned} v_k(t) = {} & \theta * D * \log_{10}(pH\,\text{Rand}_1) * v_k + \log_{10} * (pH\,\text{Rand}_1) \\ & * \log_{10}(\text{Temp Rand}_2) * \left(x_{\text{best}_k} - x_k(t)\right) + \log_{10} \\ & * (pH\,\text{Rand}_1) * \log_{10}(\text{Temp Rand}_2) * \left(x_{g\text{best}_k} - x_k(t)\right), \end{aligned} \tag{29}$$

where D is the damping factor can vary randomly between 0 and 1, pH Rand_1 is a random number [7, 14] that shows the pH value, Temp Rand_2 is the random temperature [35.1 to 38.5] of visited location, x_{best_k} and $x_{g\text{best}_k}$ are the personal best position of k^{th} sperm, t is the iteration number, and θ can be given by following equation:

$$\theta(t+1) = \mu * \theta(t) * (1 - \theta(t)) 0 \leq \theta \leq 1, \tag{30}$$

where μ is a control parameter and can vary between 0 and 4. The detailed modelling of this algorithm can be seen in [41].

4. Results and Discussion

MOSSA based multiobjective congestion management have been evaluated on IEEE 30-bus [23] system and IEEE 118 [23] bus system. To manage congestion, demand response and wind plant-based distributed generation have been employed. The obtained results of the proposed approach have also been compared with reported results in literature [23, 38]. Simulations have been performed using MATLAB platform.

4.1. IEEE 30 Bus-System. This bus system consists of 6 generator buses (at bus no. 1, 2, 13, 22, 23, and 27), 24 load buses and 41 transmission lines [38]. Base case results of transmission line flows employing Newton Raphson load flow (NRLF) have been shown in Table 2. The highly loaded lines (10, 16, and 29) have been identified as congested (critical) lines.

For applying demand response to manage transmission congestion, 7 receptive customers have been found through power transfer distribution factor [38]. These 7 load buses are, 8, 12, 17, 19, 21, and 30. In this work, load elasticity has been taken as −0.1 [42]. The market electricity price has been decided to be taken as same, before and after demand response. The cost of wind power generation has been taken as 3.75 \$/MWhr [39].

In order to explore congestion over critical lines, maximum thermal limit of 35 MVA (3-objectives-group A) and 32 MVA (2-objectives-group B) have been considered so that at least one critical line gets congested and management of that congestion could be carried out. For that only line no 10, 16, and 29 have been considered as critical lines and the power flows over other lines have been observed.

4.1.1. Group "A": 3-Objectives (35 MVA Thermal Rating). In this group, thermal rating of transmission lines has been considered as 35 MVA and multiobjective (minimization of overall cost, minimization of CO2 emission and minimization of maximum line loading) CM has been carried out to mitigate congestion. For this group, generation rescheduling (GR), DR, and DG have been employed as congestion control strategies in following ways:

Strategy $A1$: Only GR.

Strategy $A2$: GR with DR.

Strategy $A3$: GR and DR along with DG.

For each strategy by having several trials of implementation of the proposed algorithm MOSSA with different population size and generations, the final best results were tried to obtain. Population size and maximum number of generations are found to be 100 and 200, respectively, for which the proposed MOSSA algorithm is producing best results. For CM while implementing MOSSA out of 100 probable solutions (population size), 70, 72, and 75 nondominated solutions were obtained for strategies A_1, A_2, and A_3, respectively.

For solving multiobjective congestion management problem, each objective function has been assigned weighting coefficient for seven specific cases. These seven specific cases have been shown in Table 3 and considered as different case studies.

Optimal solutions (optimal fronts) obtained by implementing MOSSA have been shown in Figure 2, Figure 3, and Figure 4 for strategies A_1, A_2, and A_3, respectively. Seven specific cases have also been shown in these Figures.

The optimum values of three conflicting objective functions and control variables obtained by employing MOSSA for CM have been shown in Tables 4–6.

It can be seen from Table 4 that the minimum cost, emission, and line loading obtained for strategy A_1 are 574.835 \$/hr (Case 1), 282.537 tons/hr (Case 2), and 32.2585 MVA (Case 3), respectively. Table 5 shows the best (minimum) results for cost, emission, and line loading as 573.992 \$/hr (Case 1), 259.08 tons/hr (Case 2), and 32.1767 MVA (Case 3), respectively, for strategy A_2. Similarly, for strategy A_3, best cost, emission, and line loading can be seen from Table 6 as 573.515 \$/hr (Case 1), 246.069 tons/hr (Case 2), and 26.621 MVA (Case 3), respectively.

The comparison among optimal solutions (pareto fronts) obtained for strategies A_1, A_2, and A_3 has been shown in Figure 5.

Table 7 shows the optimized power flows on transmission lines of Case 1 for strategy A_1 (group A). From this Table it is very clear that the MVA power flows over line no. 10, 16, and 29 are 34.06 MVA, 20.86 MVA, and 30.22 MVA, respectively, which are higher. Hence, these lines have been considered as critical lines (denoted by * sign). The power flows over other lines are very low as compared to thermal rating (35 MVA) therefore only critical lines have been considered for congestion management analysis.

Optimized power flows (only for highly congested lines) obtained by employing MOSSA, for all strategies of group A have been shown in Table 8. The optimum flows over line no. 10 was found to be 32.359 MVA (Case 3) for strategy A_1, 32.277 MVA (Case 3) for strategy A_2, and 26.729 MVA (Case 3) for strategy A_3.

Since pictorial representation is more effective as compared to numerals depiction, the bar chart for presenting transmission reliability margin over all three congested lines for all three strategies has been shown in Figure 6.

Observation.

(1) The optimum location of DG (RIPP) has been found, bus no. 8, which is suppling 30 MW maximum load.

Table 2: Transmission line flows (MVA) after NRLF.

Line no.	From bus	To bus	NRLF (MVA)	Line no.	From bus	To bus	NRLF (MVA)
1	1	2	12.09	22	15	18	9.2
2	1	3	16.08	23	18	19	5.88
3	2	4	17.39	24	19	20	5.28
4	3	4	13.3	25	10	20	7.51
5	2	5	15.05	26	10	17	8.69
6	2	6	21.99	27	10	21	11.99
7	4	6	25.22	28	10	22	9.42
8	5	7	15.31	29*	21	22	30.51
9	6	7	10.11	30	15	23	10.46
10*	6	8	34.83	31	22	24	8.1
11	6	9	6.74	32	23	24	7.14
12	6	10	3.84	33	24	25	4.27
13	9	11	0	34	25	26	4.27
14	9	10	6.77	35	25	27	7.54
15	4	12	2.64	36	28	27	8.85
16*	12	13	38.7	37	27	29	6.4
17	12	14	5.46	38	27	30	7.32
18	12	15	9.55	39	29	30	3.73
19	12	16	9.27	40	8	28	8.1
20	14	15	1.17	41	6	28	2.81
21	16	17	6.08				

(2) The MVA power flow at critical transmission line no. 10 that is connected between buses 6 and 8 has been found, 26.6210 MW (strategy B3, case3).

(3) The proposed multiobjective approach of CM MOSSA has eliminated congestion efficiently over all critical lines.

(4) The congestion management performance of strategy A_3 has been found better as compared to strategy A_2 and A_1.

(5) For strategy A_3 of congestion management,

  (1) This is very clear from Tables 4–6 and Figure 5 that maximum minimization of all objective functions (individual and simultaneous) has been achieved.
  (2) It is very clear from Table 8 that maximum optimized power flows have been found.
  (3) Figure 6 distinctly shows the highest transmission reliability margin for strategy A_3.

(6) All above facts not only appreciate the use of DR for managing congestion but also indicates the importance of adding distributed generation (RIPP) along with DR.

4.1.2. Group "B": 2-Objectives (32 MVA) Thermal Rating. In this group only two objective functions (minimization of overall operational cost and minimization of CO_2 emission) have been considered for solving multiobjective optimization problem of CM. Thermal rating of transmission lines have been considered 32 MVA. In this group, congestion control strategies are taken as follows:

Strategy *B*1: only GR.

Strategy *B*2: GR with DR.

Strategy *B*3: GR and DR along with DG.

For this strategy of CM, performance of the proposed MOSSA has been compared with two nature inspired metaheuristic optimization algorithms named as multiobjective modified sperm swarm optimization and multiobjective adoptive rat swarm optimization.

The final population size and maximum number of iterations of proposed algorithm MOSSA that are producing best results for cost and emission are found to be 120 and 200. These parameters have been obtained by having several trials. In this group out of 120 probable solutions, 70, 72, and 78 nondominated solutions have been determined for strategies B_1, B_2, and B_3, respectively. After having several trials population size and the number of iteration for MMSSO and MARSO have been found 100 and 180 for strategy B_3. The optimal solutions obtained by MMSSO and MARSO are 62 and 48, respectively.

For solving 2-objective congestion management problem, each objective function has been assigned some specific values these are mentioned in Table 9. On this basis 5 specific points have been identified.

Figures 7–9 show the optimal solutions (pareto fronts) obtained by MOSSA for strategy B_1, B_2, and B_3, respectively. Out of these nondominated solutions, five specific cases given in Table 9 have been recognized and marked on these pareto-optimal fronts.

For strategy B_3 the multiobjective congestion management has been carried out by employing multiobjective salp swarm algorithm, multiobjective modified sperm swarm optimization, and multiobjective adoptive rat swarm optimization. The pareto-optimal fronts obtained by these three algorithms have been shown in Figure 10. It is very clear from this Figure that the performance of MMSSO (shown by blue colour) is better than MARSO (shown by green colour) and the proposed MOSSA (shown by red colour) is better than MMSSO and MARSO both.

Table 3: Weighting coefficients of objective functions for Group A.

Weighting coefficients	Case 1	Case 2	Case 3	Case 4	Case 5	Case 6	Case 7
Cost	1	0	0	0.333	0.5	0.5	0
Emission	0	1	0	0.333	0	0.5	0.5
Line loading	0	0	1	0.333	0.5	0	0.5

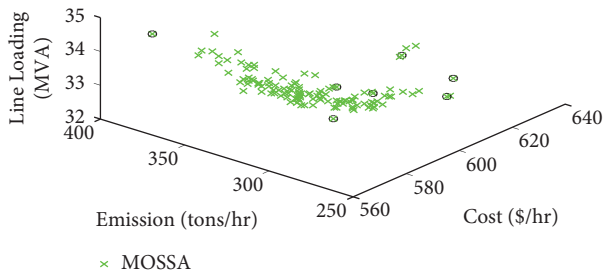

Figure 2: Pareto-optimal front for strategy A_1.

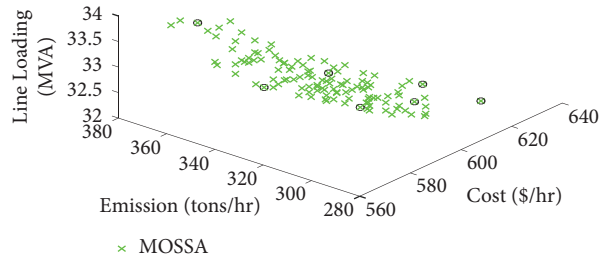

Figure 3: Pareto-optimal front for strategy A_2.

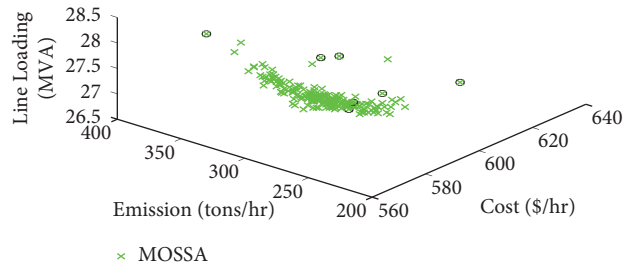

Figure 4: Pareto-optimal front for strategy A_3.

For CM the results (optimal control variables and objective function values) obtained by employing MOSSA have been shown in Tables 10–12. It can be seen from Table 10 that the minimum cost and emission obtained for strategy B_1 are 578.083 \$/hr (Case 1) and 285.162 tons/hr (Case 5), respectively. Table 11 shows the best (minimum) results for cost and emission as 576.083 \$/hr (Case 1) and 283.162 tons/hr (Case 5), respectively, for strategy B_2. Similarly, for strategy B_3, best cost and emission can be seen from Table 12 as 574.582 \$/hr (Case 1) and 262.312 tons/hr (Case 5), respectively.

Optimized power flows over highly congested lines for all strategies of group B have been shown in Table 13. The optimized power flow over line no.10 for strategy B_1 is found to be 31.850 MVA (Case 3), for strategy B_2 is 31.783 MVA (Case 1), and for strategy B_3 is 28.065MVA (Case 3).

The percentage transmission reliability margins have been calculated with respect to imposed thermal limit over lines. This enhancement of TRM in terms of percentage improvement has been shown in Figure 11 for all strategies of group B.

Observations.

(1) Congestion control strategies B_1, B_2, and B_3 all possess same thermal limit but Tables 10–12 clearly shows that the cost and emission both found better in strategy B_3.

(2) Figure 10 indicates better performance of MOSSA as compared to MMSSO and MARSO both for congestion control strategy B_3.

(3) It can be seen from Table 13 that the optimum power flow over transmission line no. 10 has remarkably reduced for strategy B_3 as compared to strategies B_1 and B_2.

(4) It is clear from Figure 11 that the reliability margin is strategy in B_3 is higher as compared to other two schemes B_1 and B_2.

(5) This clearly establishes the significance of implementation of DG along with DR towards managing congestion.

The proposed approach of CM has been compared with reported methods [23, 38] on the basis of result obtained. This comprehensive comparison has been presented in Table 14. This comparison has been carried out for the same power system i.e., IEEE 30-bus system. Line thermal limits have been considered as 32 and 35 MVA, which are taken by the proposed approach and [23], while a thermal limit of 32 MVA has been considered by [38]. For comparison "various control strategies to manage congestion have been considered. The strategies of this paper have been compared to scenarios of [23]. The strategy B_1 has been compared with [38]. In Table 14 NA has been mentioned for "not applicable" cases.

4.2. IEEE 118-Bus System. For congestion management the proposed approach has also been evaluated on a big power system i.e., IEEE 118-bus system This system comprises of 99 load buses, 54 generator buses, and 186 transmission lines. Bus no. 69 is the reference bus. The details of this system have been taken from [23]. To create congestion in transmission line 20% load has been increased at each load bus. Consequently, apparent power flows over congested transmission lines (shown in Table 15) have been found higher as compared to their thermal ratings. Hence, these lines have been considered as critical lines.

Table 4: Optimized variables for strategy A_1.

	Case 1	Case 2	Case 3	Case 4	Case 5	Case 6	Case 7
PG1 (MW)	43.7198	23.7009	33.9880	15.0111	12.6597	29.443	21.7909
PG2 (MW)	58.0385	27.9200	28.5690	44.5739	50.18395	43.901	26.8511
PG3 (MW)	17.5183	30.3000	17.9940	21.6091	22.46501	25.134	30.8579
PG4 (MW)	23.2818	33.9900	29.6340	27.2758	27.30774	27.184	27.8138
PG5 (MW)	17.0351	30.0000	27.8390	29.9310	24.48725	25.315	29.7888
PG6 (MW)	32.0964	45.3800	54.1522	53.6945	54.9160	40.461	54.9710
Cost ($/hr)	574.835	618.610	634.705	608.319	606.426	588.468	620.637
Emission (tons/hr)	392.922	282.537	338.603	314.062	332.708	306.550	289.657
Loading (MVA)	34.4487	33.0015	32.2585	32.410	32.3946	32.462	32.2720

Table 5: Optimized variables for strategy $A2$.

	Case 1	Case 2	Case 3	Case 4	Case 5	Case 6	Case 7
PG1 (MW)	43.5526	21.6270	13.8319	23.4974	35.0322	34.2738	22.0440
PG2 (MW)	57.9636	28.3000	32.7507	38.4763	47.2010	37.6521	27.5273
PG3 (MW)	17.5627	29.1550	32.5603	26.7211	12.7673	25.0027	30.8975
PG4 (MW)	23.1682	29.4760	28.2103	25.4307	23.8391	26.0210	30.4195
PG5 (MW)	17.1340	27.5300	29.1842	24.5753	20.8146	21.6609	25.9777
PG6 (MW)	31.8561	43.7430	54.999	52.7836	52.1044	46.7551	54.5817
DR1 (MW)	0.01400	2.71400	0.03871	0.04414	0.09760	0.06407	0.05061
DR2 (MW)	0.12980	2.65000	0.14973	0.14949	0.14918	0.14630	0.14894
DR3 (MW)	0.05590	1.6560	0.04151	0.04681	0.04763	0.04431	0.05490
DR4(MW)	0.04500	0.65210	0.04459	0.04418	0.03840	0.04099	0.04325
DR5 (MW)	0.04750	0.84750	0.04622	0.04635	0.04625	0.04208	0.04518
DR6 (MW)	0.08750	1.58750	0.08733	0.08686	0.08377	0.08394	0.07020
DR7 (MW)	0.05290	0.95300	0.05292	0.05283	0.05284	0.05167	0.05070
Cost ($/hr)	573.992	590.449	623.454	599.692	584.2237	589.044	617.512
Emission (tons/hr)	390.979	249.080	296.132	298.334	341.9832	305.433	288.365
Loading (MVA)	34.3450	32.8282	32.1767	32.4611	32.6500	32.9760	32.2386

Table 6: Optimized variables for strategy A_3.

	Case 1	Case 2	Case 3	Case 4	Case 5	Case 6	Case 7
PG_1 (MW)	41.9537	22.3561	7.88271	26.7761	31.8125	34.6170	29.4501
PG_2 (MW)	56.0665	28.2654	55.8093	40.8436	43.5050	41.6306	32.5137
PG_3 (MW)	15.9938	31.0410	0.17731	20.7206	14.9278	20.4578	26.3910
PG_4 (MW)	22.7649	29.9999	31.0209	25.3998	24.0778	24.1703	23.7110
PG_5 (MW)	15.6768	29.3696	29.9986	20.0396	17.7021	22.6858	20.8522
PG_6 (MW)	28.7343	41.8194	54.9999	45.3554	49.3696	37.7765	48.7966
DR_1 (MW)	0.05370	0.11398	0.02961	0.09594	0.11080	0.07960	0.10150
DR_2 (MW)	0.12990	0.14989	0.15000	0.14981	0.14970	0.10600	0.02090
DR_3 (MW)	0.03590	0.05591	0.03697	0.04426	0.04960	0.05580	0.01480
DR_4 (MW)	0.01490	0.04498	0.03211	0.04287	0.04460	0.02550	0.02140
DR_5 (MW)	0.04750	0.04744	0.04726	0.04686	0.04500	0.03170	0.02770
DR_6 (MW)	0.08740	0.08747	0.07998	0.07983	0.08720	0.07060	0.01270
DR_7 (MW)	0.03070	0.05297	0.05295	0.05229	0.05250	0.04860	0.02230
P_{RIPP} (MW)	10.0000	10.0000	9.81780	9.97090	9.99210	9.84240	9.79230
Cost ($/hr)	573.515	615.778	623.207	587.785	584.056	582.246	596.118
Emission (tons/hr)	358.259	246.069	358.668	271.466	298.368	286.632	269.167
Loading (MVA)	28.1235	27.1604	26.6210	27.1230	27.7582	28.4353	27.8879

To relieve overloading of these critical transmission lines multiobjective (minimization of overall cost and CO_2 emission) CM has been carried out. Demand response along with RIPP has been employed to manage congestion. Customers at bus number 6, 32, 45, 62, 77, and 78 (sensitive buses) take part in DR. 10% reduction in demand has been considered.

The maximum capacity of wind plant has been considered, 10 MW (individual). For CM in a big power system optimum location of wind plant (RIPP) have been found at bus number 59, 90, and 116.

For managing congestion as multiobjective optimization problem, the proposed MOSSA has obtained 80 pareto-optimal solutions out of 200 probable solutions.

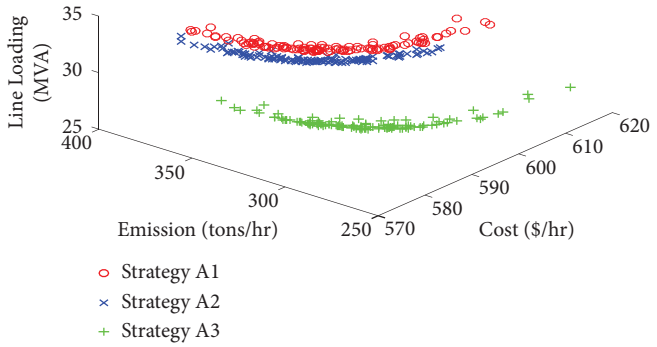

Figure 5: Comparison of pareto-optimal fronts for all strategies of group A.

Table 7: Optimized power flow for case 1 strategy A_1 of group A.

Line no.	Power flow (MVA)	Line no.	Power flow (MVA)	Line no.	Power flow (MVA)	Line no.	Power flow (MVA)
1	21.04	11	11.11	21	3.59	31	5.16
2	20.55	12	6.38	22	8.06	32	3.12
3	19.24	13	0.00	23	4.76	33	11.46
4	18.16	14	11.27	24	5.63	34	4.22
5	14.33	15	19.23	25	7.97	35	15.81
6	21.83	16*	20.86	26	7.75	36	25.06
7	18.44	17	5.10	27	12.44	37	6.32
8	14.26	18	6.83	28	9.88	38	7.18
9	12.40	19	7.27	29*	30.22	39	3.71
10*	34.06	20	1.60	30	11.34	40	10.38
						41	14.98

Table 8: Optimized power flow for all strategies of group A.

Strategy	Line no.	Optimum power flows in MVA						
		Case 1	Case 2	Case 3	Case 4	Case 5	Case 6	Case 7
A_1	10	34.061	33.057	32.359	32.451	32.755	33.339	32.404
	16	20.864	31.745	25.207	24.086	18.090	24.794	32.100
	29	30.224	34.109	34.586	32.763	30.818	32.285	33.682
A_2	10	34.058	32.993	32.277	32.505	32.540	33.567	32.353
	16	21.268	29.611	26.935	23.499	15.697	26.310	28.385
	29	30.739	34.761	31.508	32.712	30.779	32.114	33.823
A_3	10	28.189	27.165	26.729	26.979	26.980	28.435	27.888
	16	20.458	26.584	30.39	22.828	19.343	23.516	28.554
	29	29.810	33.050	31.362	31.700	30.691	31.219	31.653

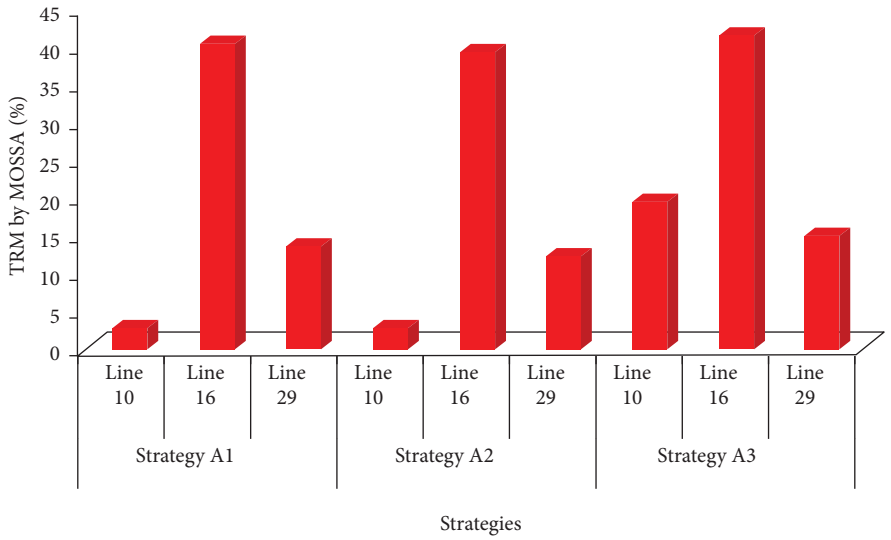

Figure 6: Percentage Improvement in TRM over critical lines for group A.

Table 9: Weighting coefficients of objective functions for group B.

Weighting coefficients	Case 1	Case 2	Case 3	Case 4	Case 5
Cost	1	0.75	0.5	0.25	0
Emission	0	0.25	0.5	0.75	1

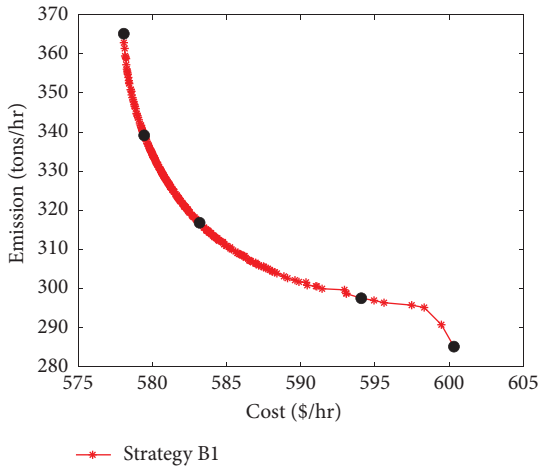

Figure 7: Pareto-optimal front for strategy B_1.

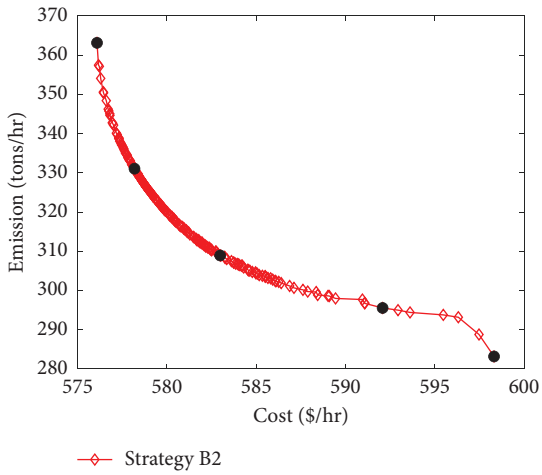

Figure 8: Pareto-optimal front for strategy B_2.

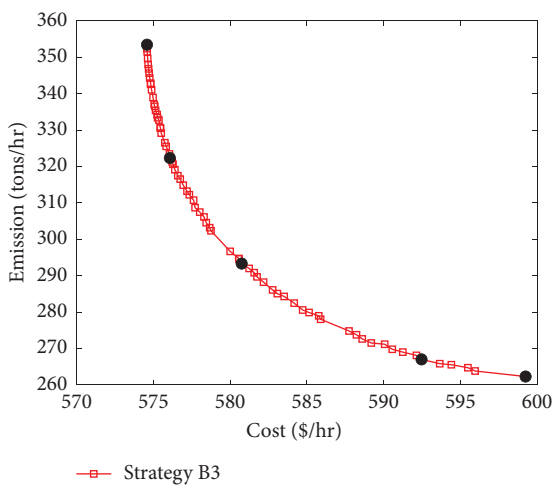

Figure 9: Pareto-optimal front for strategy B_3.

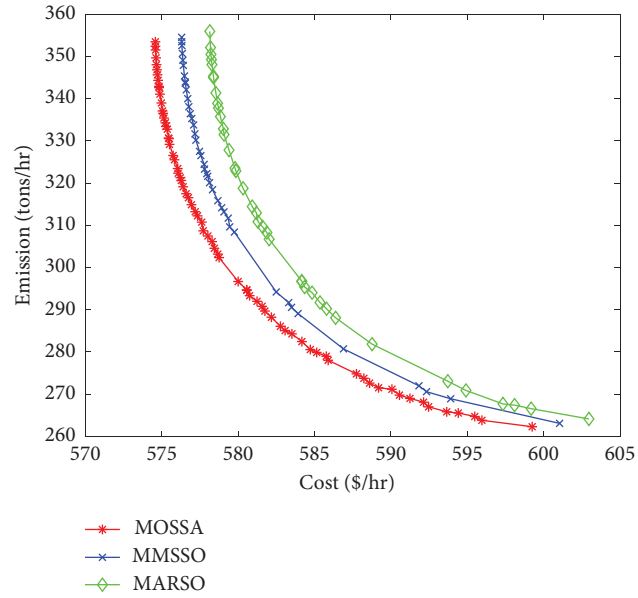

Figure 10: Comparison of pareto-optimal fronts obtained by MOSSA, MMSSO, and MARSO for strategy B_3.

Table 10: Optimized variables for strategy B_1.

	Case 1	Case 2	Case 3	Case 4	Case 5
PG_1 (MW)	40.6248	36.8392	33.7121	30.86823	26.9647
PG_2 (MW)	52.1025	48.2657	42.6211	38.1611	31.2577
PG_3 (MW)	15.5081	18.0972	21.7771	26.5776	29.8260
PG_4 (MW)	22.6525	23.4522	24.0100	22.2285	22.9801
PG_5 (MW)	17.2059	18.6179	22.1601	24.5549	29.9999
PG_6 (MW)	44.0640	46.8016	47.6911	49.6036	51.0395
Cost ($/hr)	578.083	579.455	583.188	594.077	600.318
Emission (tons/hr)	365.149	339.162	316.825	297.529	285.162

Table 11: Optimized variables for strategy B_2.

	Case 1	Case 2	Case 3	Case 4	Case 5
PG_1 (MW)	40.0462	35.6668	32.5827	30.4569	26.5898
PG_2 (MW)	53.3835	47.1553	41.0912	35.9461	31.2685
PG_3 (MW)	15.1985	18.6812	22.8518	28.8938	29.8184
PG_4 (MW)	22.2794	23.2709	23.4526	22.1072	23.1169
PG_5 (MW)	15.0985	19.1535	22.9591	24.9177	29.8332
PG_6 (MW)	45.0264	47.6911	48.5970	49.1907	49.1780
DR_1 (MW)	0.12000	0.09080	0.09064	0.08974	0.29100
DR_2 (MW)	0.22000	0.11988	0.11988	0.11988	0.62000
DR_3 (MW)	0.04470	0.04444	0.04441	0.04310	0.44800
DR_4 (MW)	0.03600	0.03570	0.03556	0.03560	0.43660
DR_5 (MW)	0.03800	0.03768	0.03770	0.03789	0.03800
DR_6 (MW)	0.06990	0.06971	0.06961	0.06957	0.37000
DR_7 (MW)	0.04240	0.04209	0.04208	0.04225	0.04240
Cost ($/hr)	576.083	578.182	582.98	592.077	598.318
Emission (tons/hr)	363.149	331.053	308.922	295.529	283.162

Table 12: Optimized variables for strategy B_3.

	Case 1	Case 2	Case 3	Case 4	Case 5
PG_1 (MW)	41.4384	37.6888	34.5542	28.8564	25.3077
PG_2 (MW)	55.2727	50.6613	43.8625	36.1831	34.1679
PG_3 (MW)	16.4279	19.0460	20.7747	25.1611	29.4997
PG_4 (MW)	22.7588	23.7090	23.7595	24.0603	23.8601
PG_5 (MW)	16.3997	18.1523	20.2731	25.1039	25.2513
PG_6 (MW)	29.3348	32.2188	38.2543	42.1407	43.3897
DR_1 (MW)	0.06834	0.06695	0.06499	0.06378	0.06165
DR_2 (MW)	0.05958	0.05503	0.05247	0.03428	0.03577
DR_3 (MW)	0.02362	0.03193	0.02706	0.02256	0.02064
DR_4 (MW)	0.02503	0.02441	0.02495	0.02278	0.02669
DR_5 (MW)	0.01975	0.01662	0.02118	0.01509	0.01534
DR_6 (MW)	0.05132	0.04862	0.03764	0.03477	0.03407
DR_7 (MW)	0.01260	0.03153	0.02253	0.02117	0.02368
P_{WP} (MW)	9.88000	9.98000	9.89000	9.89000	9.89000
Cost ($/hr)	574.582	576.071	580.749	592.464	599.243
Emission (tons/hr)	353.437	322.327	293.331	267.017	262.312

Table 13: Optimized MVA power flows over critical lines for all strategies of group B.

Strategy	Line no.	Case 1	Case 2	Case 3	Case 4	Case 5
B_1	10	31.850	31.840	31.780	31.730	31.710
	16	19.540	21.590	24.730	28.900	31.720
	29	30.720	31.280	31.68	31.77	31.220
B_2	10	31.783	31.122	31.003	31.762	31.678
	16	19.924	20.918	24.076	27.892	28.553
	29	30.108	31.259	31.931	31.980	31.988
B_3	10	28.065	28.862	28.457	28.228	28.083
	16	19.797	22.788	24.147	27.973	30.775
	29	29.774	30.325	31.646	31.891	31.989

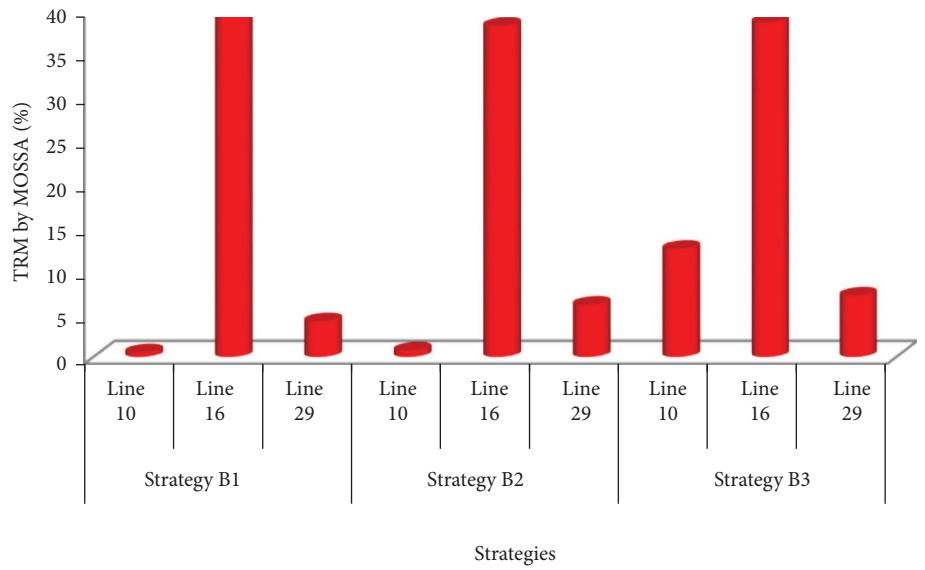

Figure 11: Percentage Improvement in TRM over critical lines for Group B.

Three specific cases by giving individual weightage to each objective function have been mentioned in Table 16.

The Pareto-optimal front obtained by MOSSA has been drawn in Figure 12 and three specific cases (Case 1, Case 2, and Case 3) have been marked in Figure 12.

The optimized apparent power flows over critical lines (line no. 5, 41, 62, 92, and 121) have been shown in Table 16. This table also shows the base case apparent power flows, thermal ratings, and overloading of the 5 critical lines. A remarkable observation of this Table is that the proposed

Table 14: Result comparison between proposed approach and reported methods [23, 38].

S. No.`	Line thermal rating (MVA)	Method	Best solution Cost ($/hr)	Best solution Emission (tons/hr)	Line loading (MVA)	Preferred solution Cost ($/hr)	Preferred solution Emission (tons/hr)	Optimal flow (MVA)	DR (MW)	DG (MW)
1	35	MOPSO (scenario 1) [23]	574.870	282.590	NA	585.32	311.040	34.22	NA	NA
		MOSSA (strategy A_1)	574.835	282.537	32.258	588.47	306.550	34.061	NA	NA
2	35	MOPSO (scenario 2) [23]	574.020	249.250	NA	623.57	277.120	34.15	0.44	NA
		MOSSA (strategy A_2)	573.992	249.080	32.18	589.04	305.430	34.058	0.4326	NA
		MOSSA (strategy A_3)	573.515	246.069	26.62	582.25	286.632	28.189	0.40	10
3	32	BF-NM [29]	648.860	NA	NA	NA	NA	NA	NA	NA
		MOPSO (scenario 3) [23]	579.180	285.440	NA	588.33	307.800	31.99	NA	NA
		MOSSA (strategy B_1)	578.083	285.162	NA	583.188	316.825	31.85	NA	NA
4	32	MOPSO (scenario 4) [23]	577.900	250.180	NA	624.80	278.270	31.96	0.6	NA
		MOSSA (scenario B_2)	576.083	283.162	NA	580.98	308.922	31.783	0.571	NA
		MOSSA (strategy B_3)	574.582	262.312	NA	580.749	293.331	28.065	0.260	9.88

Table 15: Weighting coefficients of objective functions for IEEE 118-bus system.

Objective function	Case 1	Case 2	Case 3
Cost	1	0.5	0
Emission	0	0.5	1

Table 16: Power flows of case 1 for IEEE 118-bus system.

Line no	From bus	To bus	Base case (MVA PF)	Thermal line rating	Without CM	After CM
5	5	6	88.05	132.07	140.87	136.90
41	23	32	91.77	137.65	146.82	129.46
62	45	46	36.71	55.07	58.74	55.89
92	61	62	28.83	43.24	46.13	40.69
121	77	78	45.91	68.87	73.46	63.00

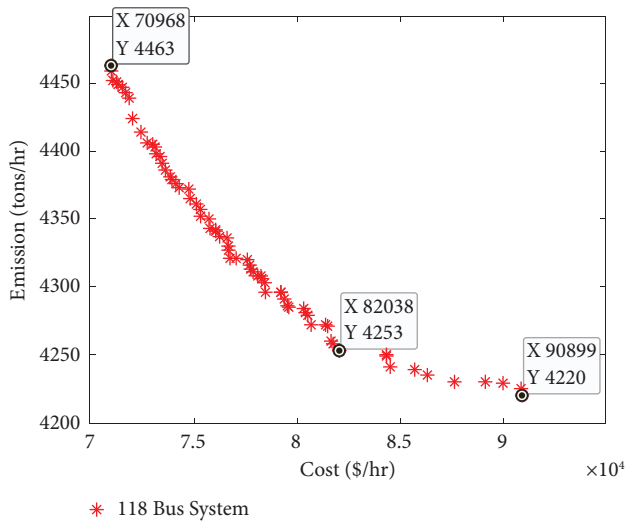

Figure 12: Pareto-optimal fronts obtained for IEEE 118-bus system.

Table 17: Optimized parameters for IEEE 118-bus system.

	DR (MW)	RIPP (MW)	DR cost ($/hr)	RIPP cost ($/hr)	Fuel cost ($/hr)	Cost ($/hr)	Emission (tons/hr)
Case 1	5.9345	26.89	40.82936	100.8375	70826.33	70968	4463
Case 2	6.8845	26.02	47.36536	97.575	81893.06	82038	4253
Case 3	8.6543	25.440	59.54184	95.4	90750.06	90899	4220

Table 18: Nomenclature.

a_i, b_i and c_i	Cost coefficients of i^{th} thermal generating unit
α_i, β_i and γ_i	Emission coefficients of i^{th} thermal generating unit
C_G	Generation cost for thermal generators ($/hr)
$P_{G_i}^{\min}$ and $P_{G_i}^{\max}$	Minimum and maximum active power limit of i^{th} generating unit (MW)
$Q_{G_i}^{\min}$ and $Q_{G_i}^{\max}$	Minimum and maximum reactive power limit of i^{th} generating unit (MVAR)
P_{G_i}	Active power generated by i^{th} generating unit (MW
Q_{G_i}	Reactive power generated by i^{th} generating unit (MVAR)
P_{D_i}	Active power demand at i^{th} load bus (MW)
Q_{D_i}	Reactive power demand at i^{th} load bus (MVAR)
$V_{G_i}^{\min}$ and $V_{G_i}^{\max}$	Minimum and maximum voltage limits of i^{th} generating unit (volt)
N_G	Total number of generators
N_{BR}	Total number of transmission lines
N_B	Total number of total buses
N_{LB}	Total number of load buses
C_{RIPP}	Cost of power generated by wind power plant as renewable independent power producer ($/hr)
P_{WP}	Active power generated by wind plant (MW)
$P_{WP}^{\min}$ and $P_{WP}^{\max}$	Minimum and maximum power generated by wind plant (MW)
C_{DR}	Total demand response cost ($/hr)
d_{0_k}	Initial demand of k^{th} receptive customer (MW)
d_k	Reduced demand of k^{th} receptive customer (MW)
$\mu_k^{\min}$ and $\mu_k^{\max}$	Minimum and maximum incentive paid to k^{th} receptive customer
EP_0 and EP_{DR}	Electricity prices in *$/hr* before and after demand response program
$DR_k^{\min}$ *and* $DR_k^{\max}$	Minimum and maximum demand reduction of k^{th} receptive customer
ϵ	Self-elasticity of customer demand
INC	Incentive rate at which incentive paid to the receptive costumers ($/MWhr)
PEN	Penalty rate at which penalty is imposed on defaulter customers ($/hr)
LR_k	Contracted load reduction of k^{th} receptive customer (MW)
μ_k	Incentive in *$/hr* paid to the k^{th} responsive customer
$\mathscr{L}_k$	Penalty paid by k^{th} defaulter receptive customer (*$/hr*)
$V_i^{\min}$ and $V_i^{\max}$	Minimum and maximum voltage limit at i^{th} load bus (volt)
Δd_k	Change in demand of k^{th} receptive customer before and after demand response program (MW)
$S_{\max_l}$ and S_l	Maximum line loading and power flow of l^{th} transmission line (MVA)
N_{DR}	Total number of receptive customers take part in demand response
$F_i^{\min}$ and $F_i^{\max}$	Minimum and maximum value of i^{th} objective function

Table 19: Generation and emission coefficients for generators IEEE 30 bus-system.

Generator	a ($/hr)	b ($/MWhr)	c ($/MWhr^2)	(ton/hr)	(ton/MWhr)	(ton/MWhr^2)
G_1	0	2	0.02	0.04091	−0.05554	0.0649
G_2	0	1.75	0.0175	0.02543	−0.06047	0.05638
G_{13}	0	3	0.025	0.06131	−0.05555	0.05151
G_{22}	0	1	0.0625	0.04258	−0.05094	0.04586
G_{23}	0	3	0.025	0.04258	−0.05094	0.04586
G_{27}	0	3.25	0.00834	0.05326	−0.0355	0.0338

approach has eliminated the congestion over these congested lines.

Table 17 shows the optimum DR, DG as RIPP, DR cost, DG cost, and two objective functions i.e., cost and emission for three specific cases. The total operation cost for Case 1, Case 2, and Case 3 are 70968 $/hr, 82038 $/hr, and 90905 $/hr while the emission for these three cases are 4463 tons/hr, 4253 tons/hr, and 4225 tons/hr, respectively. For managing congestion optimum reduction in demand (MW) and size of RIPP (MW) along with its cost ($/hr) have been

shown in Table 17. Total operation cost is the summation of fuel cost, DR cost, and RIPP cost, which also has been shown in Table 17 for all three specific cases.

The results obtained by proposed approach have been compared with reported [23] results. The proposed approach has handled the problem of congestion as multiobjective optimization while reported method [23] has considered only one objective function i.e., cost. Total operation cost and demand response cost obtained by the proposed approach are 70968 $/hr and 40.82936 $/hr, while in reported results, total operation cost and demand response cost are 71015.2 $/hr and 151 $/hr. Therefore, the proposed approach has provided congestion management with lower operation cost and DR cost.

5. Conclusion

In the present work CM problem has been handled as multiobjective optimization and three objective functions, minimization of overall cost, minimization of CO_2 emission, and minimization of maximum line loading, have been taken. For this purpose, multiobjective salp swarm algorithm has been proposed.

For alleviating congestion over recognized transmission lines, incentive based demand response has been implemented.

However, asking more reduction in demand may create dissatisfaction among customers. For overcoming this flaw, distributed generation using renewable independent power producer has also been employed to relieve congestion over congested lines. To show the efficacy of demand response and distributed generation in managing congestion, the whole work presented in this paper has been conducted for various control strategies framed under two groups with different thermal limits.

During the CM congestion management, important findings of this paper are cost, emission, and line loading, which have become minimum when DG has been implemented along with DR. In this strategy load curtailment has also been reduced.

The proposed MOSSA based approach of CM has been implemented on two test systems IEEE 30-bus system and IEEE 118-bus system and found better when compared with other techniques and control strategies, which are already reported in the literature. The present approach of congestion management can be employed for hybrid power market as well Table 18 and Table 19.

Appendix. A

Data Availability

The data will be available on request. For the data related queries, kindly contact to Baseem Khan, baseem.khan04@gmail.com.

Conflicts of Interest

The authors declare that they have no conflicts of interest.

References

[1] H. Mojarrad, H. Rezaie, and H. Razmi, "Probabilistic integrated framework for AC/DC transmission congestion management considering system expansion, demand response, and renewable energy sources and load uncertainties," *International Transactions on Electrical Energy Systems*, vol. 31, no. 12, Article ID e13168, 2021.

[2] A. Narain, S. K. Srivastava, and S. N. Singh, "Congestion management approaches in restructured power system: key issues and challenges," *The Electricity Journal*, vol. 33, Article ID 106715, 2020.

[3] A. Pillay, S. Prabhakar Karthikeyan, and D. P. Kothari, "Congestion management in power systems–A review," *International Journal of Electrical Power & Energy Systems*, vol. 70, pp. 83–90, 2015.

[4] S. S. Reddy and S. A. Wajid, "Swarm intelligent-based congestion management using optimal rescheduling of generators," *International Journal of Bio-Inspired Computation*, vol. 13, pp. 159–168, 2019.

[5] A. Agrawal, S. N. Pandey, L. Srivastava et al., "Hybrid deep neural network-based generation rescheduling for congestion mitigation in spot power market," *IEEE Access*, vol. 10, pp. 29267–29276, 2022.

[6] S. Namilakonda and Y. Guduri, "Chaotic darwinian particle swarm optimization for real-time hierarchical congestion management of power system integrated with renewable energy sources," *International Journal of Electrical Power & Energy Systems*, vol. 128, Article ID 106632, 2021.

[7] A. Sharma and S. K. Jain, "Gravitational search assisted algorithm for TCSC placement for congestion control in deregulated power system," *Electric Power Systems Research*, vol. 174, Article ID 105874, 2019.

[8] A. Dini, A. Hassankashi, S. Pirouzi, M. Lehtonen, B. Arandian, and A. A. Baziar, "A flexible-reliable operation optimization model of the networked energy hubs with distributed generations, energy storage systems and demand response," *Energy*, vol. 239, Article ID 121923, 2022.

[9] M. Behrangrad, "A review of demand side management business models in the electricity market," *Renewable and Sustainable Energy Reviews*, vol. 47, pp. 270–283, 2015.

[10] M. Zakaryaseraji and A. Ghasemi-Marzbali, "Evaluating congestion management of power system considering the demand response program and distributed generation," *International Transactions on Electrical Energy Systems*, vol. 2022, Article ID 5818757, 13 pages, 2022.

[11] J. Gao, Z. Ma, Y. Yang, F. Gao, G. Guo, and Y. Lang, "The impact of customers' demand response behaviors on power system with renewable energy sources," *IEEE Transactions on Sustainable Energy*, vol. 11, no. 4, pp. 2581–2592, 2020.

[12] R. Alasseri, A. Tripathi, T. Joji Rao, and K. J. Sreekanth, "A review on implementation strategies for demand side management (DSM) in Kuwait through incentive-based demand response programs," *Renewable and Sustainable Energy Reviews*, vol. 77, pp. 617–635, 2017.

[13] V. K. Prajapati and V. Mahajan, "Demand response based congestion management of power system with uncertain renewable resources," *International Journal of Ambient Energy*, vol. 43, pp. 103–116, 2019.

[14] J. Wu, B. Zhang, and Y. Jiang, "Optimal day-ahead demand response contract for congestion management in the deregulated power market considering wind power," *IET Generation, Transmission & Distribution*, vol. 12, pp. 917–926, 2018.

[15] S. Suganthi, D. Devaraj, K. Ramar, and S. Hosimin Thilagar, "An improved differential evolution algorithm for congestion management in the presence of wind turbine generators," *Renewable and Sustainable Energy Reviews*, vol. 81, pp. 635–642, 2018.

[16] E. Nematbakhsh, R.-A. Hooshmand, and R. Hemmati, "A new restructuring of centralized congestion management focusing on flow-gate and locational price impacts," *International Transactions on Electrical Energy Systems*, vol. 28, no. 2, Article ID e2482, 2018.

[17] A. S. Siddiqui, A. S. Siddiqui, and A. Saxena, "Optimal intelligent strategic LMP solution and effect of DG in deregulated system for congestion management," *International Transactions on Electrical Energy Systems*, vol. 31, no. 11, Article ID e13040, 2021.

[18] D. Asija and P. Choudekar, "Congestion management using multi-objective hybrid DE-PSO optimization with solar-ess based distributed generation in deregulated power Market," *Renewable Energy Focus*, vol. 36, pp. 32–42, 2021.

[19] R. Peesapati, V. K. Yadav, and N. Kumar, "Flower pollination algorithm based multi-objective congestion management considering optimal capacities of distributed generations," *Energy*, vol. 147, pp. 980–994, 2018.

[20] Y. Wang, Y. Huang, Y. Wang, F. Li, Y. Zhang, and C. Tian, "Operation optimization in a smart micro-grid in the presence of distributed generation and demand response," *Sustainability*, vol. 10, no. 3, p. 847, 2018.

[21] E. Luo, P. Cong, H. Lu, and Y. Li, "Two-stage hierarchical congestion management method for active distribution networks with multi-type distributed energy resources," *IEEE Access*, vol. 8, pp. 120309–120320, 2020.

[22] S. M. Mousavi and T. Barforoushi, "Strategic wind power investment in competitive electricity markets considering the possibility of participation in intraday market," *IET Generation, Transmission & Distribution*, vol. 14, pp. 2676–2686, 2020.

[23] F. Zaeim-Kohan, H. Razmi, and H. Doagou-Mojarrad, "Multi-objective transmission congestion management considering demand response programs and generation rescheduling," *Applied Soft Computing*, vol. 70, pp. 169–181, 2018.

[24] S. R. Salkuti, "Multi-objective-based optimal transmission switching and demand response for managing congestion in hybrid power systems," *International Journal of Green Energy*, vol. 17, no. 8, pp. 457–466, 2020.

[25] L. Srivastava and H. Singh, "Hybrid multi-swarm particle swarm optimisation based multi-objective reactive power dispatch," *IET Generation, Transmission & Distribution*, vol. 9, no. 8, pp. 727–739, 2015.

[26] K. Zhang, Z. Wang, G. Chen et al., "Training effective deep reinforcement learning agents for real-time life-cycle production optimization," *Journal of Petroleum Science and Engineering*, vol. 208, Article ID 109766, 2022.

[27] W. Zhang, Z. Zheng, and H. Liu, "A novel droop control method to achieve maximum power output of photovoltaic for parallel inverter system," *CSEE Journal of Power and Energy Systems*, pp. 1–9, 2021.

[28] N. Huang, S. Wang, R. Wang, G. Cai, Y. Liu, and Q. Dai, "Gated spatial-temporal graph neural network based short-term load forecasting for wide-area multiple buses," *International Journal of Electrical Power & Energy Systems*, vol. 145, Article ID 108651, 2023.

[29] L. Guo, C. Ye, Y. Ding, and P. Wang, "Allocation of centrally switched fault current limiters enabled by 5G in transmission system," *IEEE Transactions on Power Delivery*, vol. 36, no. 5, pp. 3231–3241, 2021.

[30] C. Guo, C. Ye, Y. Ding, and P. Wang, "A multi-state model for transmission system resilience enhancement against short-circuit faults caused by extreme weather events," *IEEE Transactions on Power Delivery*, vol. 36, no. 4, pp. 2374–2385, 2021.

[31] C. Lu, H. Zhou, L. Li et al., "Split-core magnetoelectric current sensor and wireless current measurement application," *Measurement*, vol. 188, Article ID 110527, 2022.

[32] Y. Zhang, X. Shi, H. Zhang, Y. Cao, and V. Terzija, "Review on deep learning applications in frequency analysis and control of modern power system," *International Journal of Electrical Power & Energy Systems*, vol. 136, Article ID 107744, 2022.

[33] X. Xu, D. Niu, L. Peng, S. Zheng, and J. Qiu, "Hierarchical multi-objective optimal planning model of active distribution network considering distributed generation and demand-side response," *Sustainable Energy Technologies and Assessments*, vol. 53, Article ID 102438, 2022.

[34] H. Li, K. Hou, X. Xu, H. Jia, L. Zhu, and Y. Mu, "Probabilistic energy flow calculation for regional integrated energy system considering cross-system failures," *Applied Energy*, vol. 308, Article ID 118326, 2022.

[35] V. K. Prajapati, V. Mahajan, and N. P Padhy, "Congestion management of integrated transmission and distribution network with RES and ESS under stressed condition," *International Transactions on Electrical Energy Systems*, vol. 31, no. 2, Article ID e12757, 2021.

[36] N. Tarashandeh and A. Karimi, "Utilization of energy storage systems in congestion management of transmission networks with incentive-based approach for investors," *Journal of Energy Storage*, vol. 33, Article ID 102034, 2021.

[37] S. Mirjalili, A. H. Gandomi, S. Z. Mirjalili, S. Saremi, H. Faris, and S. M. Mirjalili, "Salp Swarm Algorithm: a bio-inspired optimizer for engineering design problems," *Advances in Engineering Software*, vol. 114, pp. 163–191, 2017.

[38] R. A. Hooshmand, M. J. Morshed, and M. Parastegari, "Congestion management by determining optimal location of series FACTS devices using hybrid bacterial foraging and Nelder–Mead algorithm," *Applied Soft Computing*, vol. 28, pp. 57–68, 2015.

[39] P. K. Tiwari, M. K. Mishra, and S. Dawn, "A two step approach for improvement of economic profit and emission with congestion management in hybrid competitive power market," *International Journal of Electrical Power & Energy Systems*, vol. 110, pp. 548–564, 2019.

[40] A. Toolabi Moghadam, M. Aghahadi, M. Eslami et al., "Adaptive rat swarm optimization for optimum tuning of SVC and PSS in a power system," *International Transactions on Electrical Energy Systems*, vol. 2022, Article ID 4798029, 13 pages, 2022.

[41] M. Eslami, B. Babaei, H. Shareef, M. Khajehzadeh, and B. Arandian, "Optimum design of damping controllers using modified Sperm swarm optimization," *IEEE Access*, vol. 9, pp. 145592–145604, 2021.

[42] A. Yousefi, T. T. Nguyen, H. Zareipour, and O. P. Malik, "Congestion management using demand response and FACTS devices," *International Journal of Electrical Power & Energy Systems*, vol. 37, no. 1, pp. 78–85, 2012.